



**Selective Detection of Ethylene Gas Using Carbon Nanotube-based Devices: Utility in Determination of Fruit Ripeness**

The MIT Faculty has made this article openly available. **Please share** how this access benefits you. Your story matters.

<b>Citation</b>	Esser, Birgit, Jan M. Schnorr, and Timothy M. Swager. "Selective Detection of Ethylene Gas Using Carbon Nanotube-based Devices: Utility in Determination of Fruit Ripeness." <i>Angewandte Chemie International Edition</i> 51.23 (2012): 5752–5756.
<b>As Published</b>	<a href="http://dx.doi.org/10.1002/anie.201201042">http://dx.doi.org/10.1002/anie.201201042</a>
<b>Publisher</b>	Wiley Blackwell
<b>Version</b>	Author's final manuscript
<b>Accessed</b>	Tue Oct 24 10:17:13 EDT 2017
<b>Citable Link</b>	<a href="http://hdl.handle.net/1721.1/74223">http://hdl.handle.net/1721.1/74223</a>
<b>Terms of Use</b>	Creative Commons Attribution-Noncommercial-Share Alike 3.0
<b>Detailed Terms</b>	<a href="http://creativecommons.org/licenses/by-nc-sa/3.0/">http://creativecommons.org/licenses/by-nc-sa/3.0/</a>

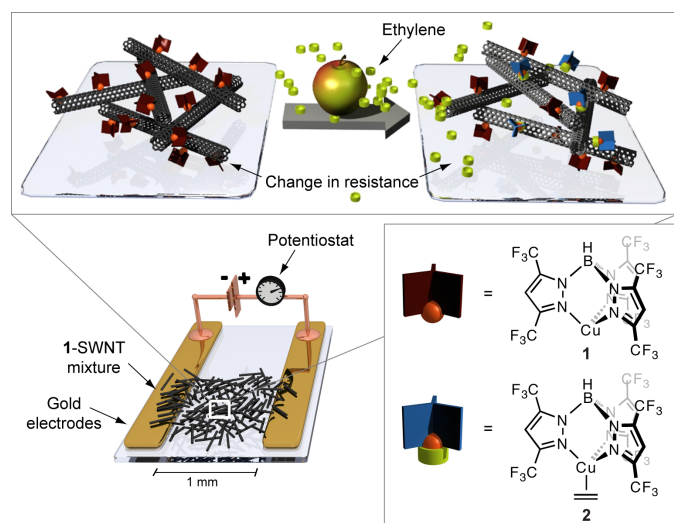
# Selective Detection of Ethylene Gas Using Carbon Nanotube based Devices: Utility in Determination of Fruit Ripeness

Birgit Esser, Jan M. Schnorr and Timothy M. Swager\*

Ethylene as the smallest plant hormone plays a role in many developmental processes in plants. For example it initiates the ripening of fruit, promotes seed germination and flowering, and is responsible for the senescence of leaves and flowers.<sup>[1]</sup> The rate-limiting step in the biosynthetic pathway to ethylene, elucidated by Yang et al., is catalysed by 1-aminocyclopropane-1-carboxylic acid (ACC) synthase.<sup>[2]</sup> Ethylene production in plants is induced during several developmental stages as well as by external factors. The ripening process is the result of ethylene binding to the receptor ETR1, which leads to the translation of ripening genes and eventually the production of enzymes that induce the visible effects of ripening. The monitoring of the ethylene concentration is of utmost importance in the horticultural industries. The internal ethylene concentration in fruit can serve as an indicator for determining the time of harvest, while the monitoring of the atmospheric ethylene level in storage facilities and during transportation is crucial for avoiding over ripening of fruit.

We herein present a reversible chemoresistive sensor able to detect sub-ppm concentrations of ethylene. Our detection scheme has high selectivity towards ethylene and is simply prepared in few steps from commercially available materials. The sensing mechanism relies on the high sensitivity in resistance of single-walled carbon nanotubes (SWNTs) to changes in their electronic surroundings. These principles have been employed in a variety of sensing applications.<sup>[3]</sup> For the selective recognition of ethylene we employ a copper(I) complex, inspired by nature, where Cu(I) has been found to be an essential cofactor of the receptor ETR1.<sup>[4]</sup> As a result of its small size and lack of polar chemical functionality, ethylene is generally hard to detect. Traditionally, ethylene concentrations are monitored through gas chromatography<sup>[5a]</sup> or laser acoustic spectroscopy,<sup>[5b]</sup> which both require expensive instrumentation and are not suitable for in-field measurements. Other techniques suggested are based on amperometric<sup>[5c]</sup> or electrochemical<sup>[5d]</sup> methods or rely on changes in luminescence properties.<sup>[5c, 6]</sup> In addition, gas-sampling tubes based on a colorimetric reaction are available.<sup>[1]</sup> The carbon nanotube based

sensing concept we have developed is shown schematically in Scheme 1. The ethylene sensitive material is an intimate mixture of SWNTs with a copper(I) complex **1** based upon a fluorinated tris(pyrazolyl) borate ligand, which is able to interact with the surface of carbon nanotubes, thereby influencing their conductivity. Upon exposure to ethylene, **1** binds to ethylene and forms complex **2**, which has a decreased interaction with the SWNT surface. The result of this transformation is an increase in resistance of the SWNT network.



Scheme 1. Schematic of ethylene detection by a chemoresistive sensor: A mixture of single-walled carbon nanotubes (SWNTs) and copper complex **1** is drop-cast between gold electrodes, and the change in resistance in response to ethylene exposure is measured. The copper complexes partly bind to ethylene molecules, resulting in a resistance change.

Our choice of the copper-ligand system **1** is based on the fact that **2** is one of the most stable copper-ethylene complexes known.<sup>[7]</sup> It is not easily oxidized under ambient conditions and is stable in high vacuum. Compound **1** has been employed in the detection of ethylene in fluorescence schemes.<sup>[6]</sup>

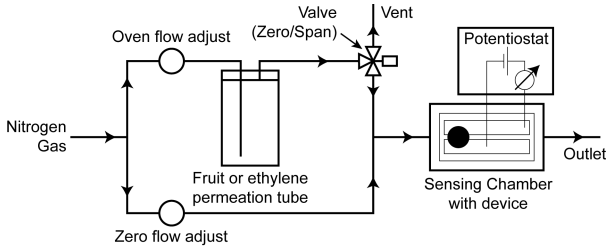
In a typical experiment **1** is ultrasonicated with SWNTs in a mixture of *o*-dichlorobenzene and toluene (2:3). Devices are prepared by drop-casting the resulting dispersion onto glass slides with pre-deposited gold electrodes (as shown in Scheme 1). The experimental setup for sensing measurements is shown in Scheme 2. The device is enclosed in a gas flow chamber, with its electrodes connected to a potentiostat. The analyte-gas mixture is produced in a gas generator, in which a stream of nitrogen gas is split into two parts, one of which is led through a flow chamber containing an ethylene permeation tube or a piece of fruit. During a measurement, a continuous gas stream of constant flow rate, which can be switched between dinitrogen and the analyte-dinitrogen mixture, is directed over the device. The results from exposing **1**-SWNT

[\*] Dr. B. Esser, J. M. Schnorr, Prof. Dr. T. M. Swager  
Department of Chemistry and Institute for Soldier  
Nanotechnologies  
Massachusetts Institute of Technology  
Cambridge, MA 02139 (USA)  
Fax: (+1) 617-253-7929  
E-mail: tswager@mit.edu

[\*\*] This research was supported (in part) by the U.S. Army Research Office under contract W911NF-07-D-0004. B. E. is grateful to the German Academy of Sciences Leopoldina for a postdoctoral fellowship (LPDS 2009-8). We thank S. L. Buchwald for the usage of computational resources, J. J. Walish for fabricating the device holder and J. G. Weis for SEM measurements.

 Supporting information for this article is available on the WWW under <http://www.angewandte.org> or from the author.

devices to low concentrations of ethylene are shown in Figure 1. We were able to detect ethylene concentrations of less than 1 ppm and performed measurements up to 50 ppm. 1 ppm is the concentration at which ripening occurs at the maximum rate for many commodities.<sup>[1]</sup> Within the range of concentrations measured (0.5 - 50 ppm), we observe a linear change in response (see Figure 1c).



**Scheme 2.** Experimental setup for sensing measurements: A continuous gas flow is directed through the device chamber. The gas stream can be switched between nitrogen gas (“Zero” mode) or the nitrogen gas analyte mixture (“Span” mode), in which the gas stream runs through the flow chamber containing the analyte (ethylene) or a piece of fruit.

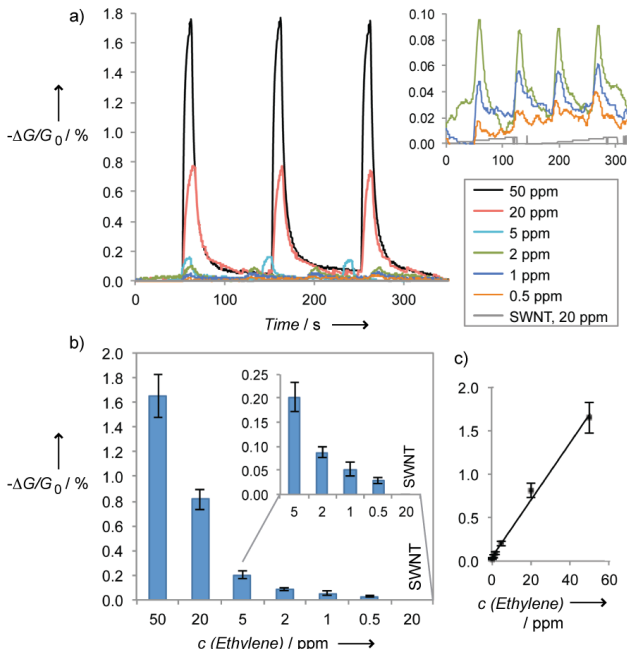


**Figure 1.** (a) Relative responses of **1**-SWNT devices to 0.5, 1, 2, 5, 20, and 50 ppm ethylene diluted with nitrogen gas and of pristine SWNT to 20 ppm ethylene (the inset<sup>8</sup> shows the responses of **1**-SWNT to 0.5, 1, and 2 ppm and of SWNT to 20 ppm); (b) average responses from three different devices each and (c) plot of average response vs. ethylene concentration.

Devices made from pristine SWNTs show no response to the same concentrations of ethylene (see Figure 1). Further controls, in which  $[\text{Cu}(\text{CH}_3\text{CN})_4]\text{PF}_6$  or the sodium equivalent of **1** (Cu replaced by Na) were employed instead of **1** did not respond to ethylene either (see SI). Employing the ethylene complex **2** resulted in device sensitivity towards 20 ppm ethylene, however, the response amounts to only ~25% of that of **1**-SWNT devices (see SI). In optimizing the ratio of **1** to SWNT we found that a large excess of **1** (ratio of **1** to SWNT carbon atoms = 1:6) resulted in the best sensitivity. We tested different types of commercially available SWNTs in our

devices (see SI). The best results were obtained with SWNTs of small diameter, namely SWNTs containing > 50% of (6,5) chirality. We assume that the stronger curvature of the carbon nanotube surface enhances the interaction between **1** and the SWNT.

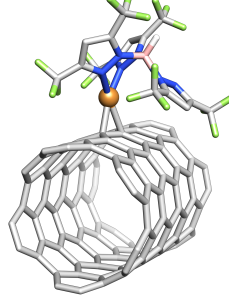


**Figure 2.** Optimized structure of **3**, in which **1** is coordinatively bound to a (6,5) SWNT fragment (B3LYP/6-31G\*, LanL2DZ for Cu; hydrogen atoms at the ends of the SWNT fragment and on the pyrazol rings have been omitted for clarity).

Upon exposure to ethylene, a reversible increase in resistance is observed. We ascribe this to a mechanism as shown in Scheme 1, where the interaction of **1** with the SWNT surface induces doping of the nanotubes. When complexes **1** bind to ethylene, this doping effect is diminished, and hence an increase in resistance is measured. In order to rationalize the interaction between **1** and the SWNT surface we performed model calculations using density functional theory. We optimized the structure of complex **3**, where the copper center in **1** is bound to the surface of a short segment of a (6,5) SWNT using the B3LYP functional with the 6-31G\* basis set for main group elements and LanL2DZ for Cu.<sup>[9]</sup> The optimized structure of **3** is shown in Figure 2. Steric interactions force one of the pyrazol rings of the ligand to be twisted in such a way that a trigonal planar coordination results for the Cu center. In an isodesmic equation, the binding strength of **1** to a (6,5) SWNT fragment (**3**) was compared to the binding in **2**. The calculation suggests that **2** is strongly favored over **3** (by 70-80 kcal/mol).<sup>[10]</sup> Since we observe reversible responses to ethylene we assume that the copper complexes **1** do not completely dissociate from the SWNTs but bind the ethylene molecules in an associative fashion.

The Raman and IR spectra of **1**-SWNT are shown in Figure 3. Upon introduction of **1** into the SWNT network a slight shift of the G and G' bands in the Raman spectrum to lower energies is observed, which can be indicative of p-type doping.<sup>[11]</sup> The IR spectrum of **1**-SWNT is dominated by the C-F stretching modes of the ligand between 1080-1260 cm<sup>-1</sup>. The ν<sub>BH</sub> shift is found at 2607 cm<sup>-1</sup>. X-ray photoelectron spectroscopy (XPS) measurements were used to confirm the ratio of **1** to SWNTs and to investigate the oxidation state of the copper centers, which can undergo oxidation to copper(II). We found a ratio of 1:22 for C<sub>SWNT</sub>:Cu (based on the Cu 2p peak, see SI for data). In high resolution scans we observed the characteristic pattern for copper(I), consisting of two peaks due to spin-orbit coupling at 932 and 952 eV.

In order to investigate the sensing mechanism, we prepared field-effect transistor (FET) devices with **1**-SWNT and pristine SWNT. A device architecture with interdigitated Au electrodes (10 μm gap) on Si with 300 nm SiO<sub>2</sub> was used. We kept the source-drain potential at a constant bias of 0.1 V, while the source-gate potential was scanned between +2 and -20 V. We observed a slight linear increase in conductance towards negative gate voltages (see SI for data), however, no strong gate effect. This lack of a measurable shift in the turn-on voltage may be the result of the fact that the charge injection

(doping) differences are very small and/or due to device geometry and the nature of the nanotube network. In those cases where strong turn-on SWNT FET responses are observed at negative gate voltages usually more highly ordered nanotube networks are employed.<sup>[12]</sup>

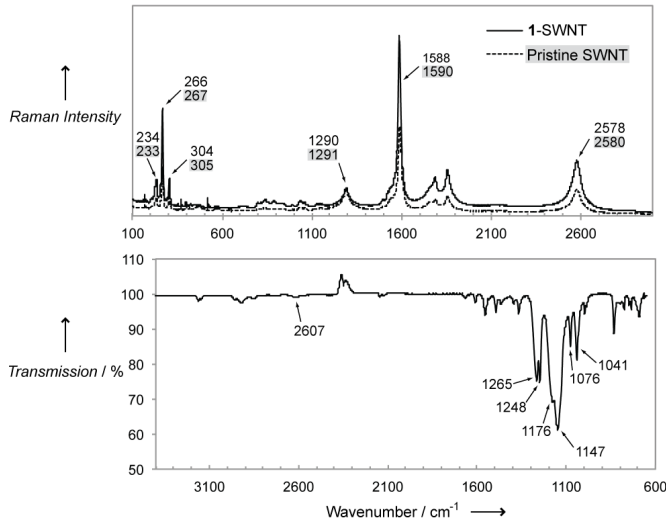


Figure 3. Top: Raman spectra of 1-SWNT and pristine SWNT (dashed line; laser energy 785 nm); bottom: IR spectrum of 1-SWNT.

We then used our sensory system to compare the ethylene emission from a selection of common fruits (banana, avocado, apple, pear, and orange). In the experimental setup, the fruit was enclosed in the gas flow chamber as shown in Scheme 2, which allowed us to expose the devices to fruit volatiles in the same way as to ethylene. The responses of 1-SWNT devices to the different fruits are shown in Figure 4a. The intensities are given in relation to the response to 20 ppm ethylene and normalized to 100 g fruit. We found the largest response for banana, followed by avocado, apple, pear, and orange. All fruit apart from orange showed ethylene concentrations above 20 ppm, which corresponds to emission rates exceeding 9,600 nL/min. In order to follow the ripening and senescing process in these fruits, we repeatedly measured their ethylene emission over several weeks (Figure 4b). Fruit can be classified into climacteric and non-climacteric fruit according to respiration rate (release of  $\text{CO}_2$ ) and  $\text{C}_2\text{H}_4$  production pattern.<sup>[1]</sup> Banana, avocado, apple, and pear belong to the climacteric group, which is characterized by a large increase in  $\text{CO}_2$  and  $\text{C}_2\text{H}_4$  production during ripening, while non-climacteric fruits, such as orange, generally show low emission rates of these gases. Once the climax (ripeness) is achieved, respiration and  $\text{C}_2\text{H}_4$  emission decrease as the fruit senesces. We were able to observe the climacteric rise during ripening in case of the pear and avocado, which showed an increased ethylene emission after the first week. For all other fruits and after the second week for the pear, measurements were conducted close to the maximum point of ripeness, and as a result our data reflects the senescence of the fruit with decreasing ethylene production rates for banana and apple. We compared two apples of the same kind and of similar ripeness, of which one was stored in a refrigerator (apple 1), while apple 2 was kept at room temperature. As anticipated, apple 2 senesced faster at room temperature, and hence its ethylene production decreased at a quicker pace than for apple 1. The orange as a non-climacteric fruit showed an overall low emission rate of ethylene.

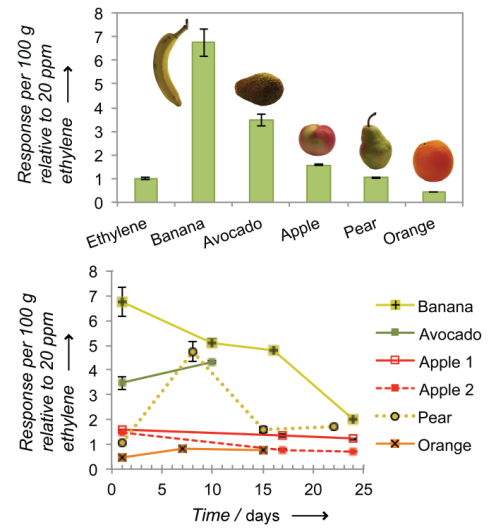


Figure 4. (a) Responses of 1-SWNT devices to 100 g of different fruit relative to 20 ppm ethylene; (b) responses to fruit monitored over several weeks.

In order to assess the selectivity of our sensory system, we measured the responses of 1-SWNT devices to several solvents (75–200 ppm concentrations) as representatives of functional groups as well as to ethanol and acetaldehyde, which occur as fruit metabolites. The results are shown in Figure 5 in comparison to the response to 50 ppm ethylene and to pristine SWNTs.

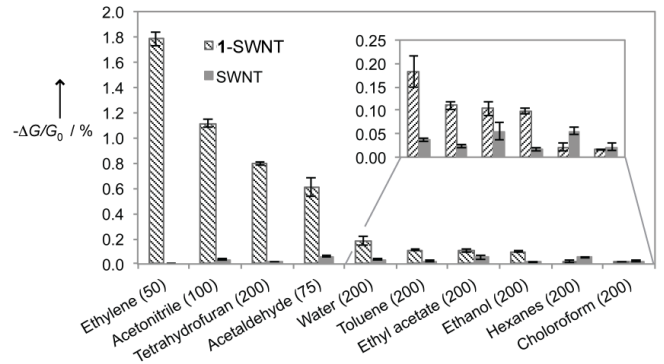


Figure 5. Relative responses of 1-SWNT devices and pristine SWNT to 50 ppm ethylene and various solvents diluted with nitrogen gas (respective concentrations are given in parentheses in ppm).

We observed significantly high responses towards acetonitrile, THF, and acetaldehyde, while all other solvents had only small effects. However, considering the concentrations of these compounds the responses are smaller in magnitude than the response to ethylene (50 ppm ethylene vs. 100 ppm acetonitrile, 200 ppm THF or 75 ppm acetaldehyde). The sensitivity of 1-SWNT devices towards these analytes is not surprising, as they are able to bind to the copper center in **1** via e.g. the nitrile group in acetonitrile or the oxygen of acetaldehyde with binding strengths comparable to that of ethylene (see SI).

The concentrations required for fruit ripening lie in most cases between 0.1 and 1 ppm, and hence in storage facilities the ethylene level is to be kept below those thresholds. Our sensory system consisting of **1** and SWNTs shows good responses down to 1 ppm of ethylene. We found that we can further improve the sensitivity by

increasing the surface area and porosity of the SWNT network structure. In order to achieve this we added 5 weight-% cross-linked polystyrene beads of 0.4–0.6  $\mu\text{m}$  diameter to the mixture, from which devices were prepared. Scanning electron microscope (SEM) images of the devices confirm a higher surface roughness for **1**-PS-SWNT devices compared to **1**-SWNT devices and the presence of SWNT bundles on the polymer beads for **1**-PS-SWNT (see SI). The responses of the resulting **1**-PS-SWNT devices to ethylene concentrations of 0.5, 1, and 2 ppm are shown in Figure 6. A 1.3–2.2 fold increase in sensitivity was observed, which we attribute to an increased surface area of the SWNT network and possibly an increase in the local ethylene concentration in the device by partitioning into the polystyrene beads.

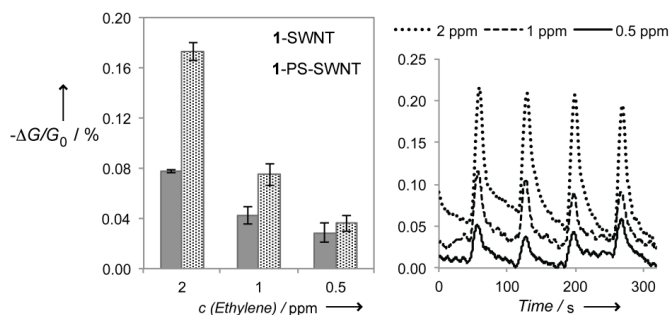


Figure 6. Comparison of the responses of **1**-SWNT devices and **1**-PS-SWNT devices to 0.5, 1, and 2 ppm ethylene.<sup>[8]</sup>

In summary, we have developed a carbon nanotube based sensor for ethylene gas, in which copper(I) complexes are employed for the specific recognition of ethylene. The sensory material is simple to prepare and allowed us to detect sub-ppm concentrations of ethylene. We further demonstrated that sensitivity can be enhanced by adding polystyrene particles. The sensory system shows good selectivity and allowed us to follow the ripening and senescing processes in different fruit.

## Experimental Section

Preparation of **1**: 8 mg (15.9  $\mu\text{mol}$ )  $[\text{CF}_3\text{SO}_3\text{Cu}]_2\cdot\text{C}_6\text{H}_6$  were dissolved in 3 mL dry, degassed toluene. 17 mg (43.5  $\mu\text{mol}$ ) hydrotris[3,5-bis(trifluoromethyl)pyrazol-1-yl]borato sodium ( $\text{Na}[\text{HB}(3,5-(\text{CF}_3)_2-\text{pz})_3]$ )<sup>13</sup> were added, and the mixture was stirred for 14 h at r.t. The reaction mixture was filtered to receive a colorless solution of **1** with a concentration of ~ 6  $\mu\text{mol}/\text{mL}$  (6 mM) (the exact concentration was determined by NMR).

Preparation of **1**-SWNT: 0.50 mg (41.6  $\mu\text{mol}$  carbon) of SWNTs (SWNT® SG65) were suspended in 0.8 mL of dry *o*-dichlorobenzene, and 1.16 mL (6.9  $\mu\text{mol}$ ) of a 6 mM solution of **1** in toluene were added. The mixture was sonicated at 30 °C for 30 min. The resulting black dispersion of **1**-SWNT was used to prepare devices.

In the case of **1**-PS-SWNT, 2.4  $\mu\text{L}$  of a suspension of cross-linked polystyrene particles in toluene (5  $\mu\text{g}/\text{mL}$ ) were added before sonication.

For further experimental details see Supporting Information.

Received: ((will be filled in by the editorial staff))  
Published online on ((will be filled in by the editorial staff))

**Keywords:** ethylene · copper · hormones · nanotubes · sensors

- [1] A. A. Kader, M. S. Reid, J. F. Thompson, in *Postharvest Technology of Horticultural Crops*, (Ed: A. A. Kader), University of California, Agricultural and Natural Resources, Publication 3311, **2002**, pp. 39 ff., 55 ff., 113 ff., 149 ff., 163 ff.
- [2] a) A. Theologis, *Cell* **1992**, *70*, 181–184; b) H. Kende, *Annu. Rev. Plant Physiol. Plant Mol. Biol.* **1993**, *44*, 283–307.
- [3] (a) D. R. Kauffman, A. Star, *Angew. Chem. Int. Ed.* **2008**, *47*, 6550–6570; (b) J. M. Schnorr, T. M. Swager, *Chem. Mater.* **2011**, *23*, 646–657.
- [4] a) F. I. Rodríguez, J. J. Esch, A. E. Hall, B. M. Binder, G. E. Schaller, A. B. Bleecker, *Science* **1999**, *283*, 996–998; b) B. M. Binder, *Plant Science* **2008**, *175*, 8–17.
- [5] a) H. Pham-Tuan, J. Vercammen, C. Devos, P. Sandra, *J. Chromatography A* **2000**, *868*, 249–259; b) M. Scotoni, A. Rossi, D. Bassi, R. Buffa, S. Iannotta, A. Boschetti, *Appl. Phys. B* **2006**, *82*, 495–500; c) L. R. Jordan, P. C. Hauser, G. A. Dawson, *Analyst* **1997**, *122*, 811–814; d) M. A. G. Zevenbergen, D. Wouters, V.-A. T. Dam, S. H. Brongersma, M. Crego-Calama, *Anal. Chem.* **2011**, *83*, 6300–6307; e) O. Green, N. A. Smith, A. B. Ellis, J. N. Burstyn, *J. Am. Chem. Soc.* **2004**, *126*, 5952–5953.
- [6] B. Esser, T. M. Swager, *Angew. Chem.* **2010**, *122*, 9056–9059; *Angew. Chem. Int. Ed.* **2010**, *49*, 8872–8875.
- [7] (a) H. V. R. Dias, H.-L. Lu, H.-J. Kim, S. A. Polach, T. K. H. H. Goh, R. G. Browning, C. J. Lovely, *Organometallics* **2002**, *21*, 1466–1473; (b) For a review on coinage metal-ethylene complexes see: H. V. R. Dias, J. Wu, *Eur. J. Inorg. Chem.* **2008**, 509–522.
- [8] The data plotted is the floating average over 5 s of the original data.
- [9] Calculations were performed using Gaussian 03 (Gaussian 03, Revision E.01, M. J. Frisch et al., Gaussian, Inc., Wallingford CT, 2004; see Supporting Information for complete citation), the B3LYP functional and as basis sets 6-31G\* for C, H, B, F, N and LanL2DZ for Cu. Minima were characterized by harmonic vibrational frequency calculations. Energetic and structural data for all optimized compounds can be found in the Supporting Information.
- [10] Due to limitations of computational power a harmonic vibrational frequency calculation could not be performed on **3**. The energy given was calculated using electronic energies.
- [11] A. Jorio, M. Dresselhaus, R. Saito, G. F. Dresselhaus, in *Raman Spectroscopy in Graphene Related Systems*, Wiley-VCH, Weinheim, Germany **2011**, pp. 327 ff.
- [12] (a) B. L. Allen, P. D. Kichambare, A. Star, *Adv. Mater.* **2007**, *19*, 1439–1451; (b) R. Martel, T. Schmidt, H. R. Shea, T. Hertel, Ph. Avouris, *Appl. Phys. Lett.* **1998**, *73*, 2447–2449; (c) S. Auvray, V. Derycke, M. Goffman, A. Filoromo, O. Jost, J.-P. Bourgois, *Nano Lett.* **2005**, *5*, 451–455.
- [13] H. V. R. Dias, W. Jin, H.-J. Kim, H.-L. Lu, *Inorg. Chem.* **1996**, *35*, 2317–2328.

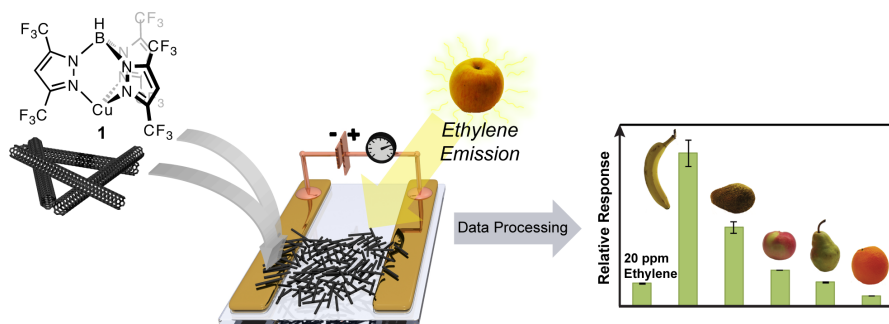
## Entry for the Table of Contents

Layout 2:

### Ethylene Detection

Birgit Esser, Jan M. Schnorr, Timothy M. Swager\* \_\_\_\_\_ Page – Page

Selective Detection of Ethylene Gas  
Using Carbon Nanotube based Devices:  
Utility in Determination of Fruit Ripeness



**Comparing Apples and Oranges:** A chemoresistive sensor for ethylene can be obtained simply by mixing copper complex **1** with single-walled carbon nanotubes. The resulting devices show sub-ppm sensitivity and high selectivity towards ethylene. The utility of the sensor was demonstrated by following ripening stages in different fruits.

## Table of Contents

1	Synthetic Procedures.....	1
1.1	General Remarks.....	1
1.1	Synthesis of 1 .....	1
1.2	Preparation of 1-SWNT .....	2
1.3	Preparation of 1-PS-SWNT .....	2
2	Device preparation .....	2
3	Sensing Measurements.....	2
4	FET measurements.....	3
5	Testing of Different SWNT Types and Control Experiments .....	4
6	Fruit Information.....	4
7	Raman Measurements, IR Measurements, and XPS Data.....	5
8	Scanning Electron Microscope Measurements .....	6
9	Isodesmic Equations .....	6
10	Electronic and zero-point vibrational energies, Cartesian coordinates.....	7
11	Complete Gaussian Citation .....	12

## 1 Synthetic Procedures

### 1.1 General Remarks

#### Materials and Synthetic Manipulations

Synthetic manipulations were carried out under an argon atmosphere using standard Schlenk techniques.  $[\text{CF}_3\text{SO}_3\text{Cu}]_2 \cdot \text{C}_6\text{H}_6$  was purchased from TCI America, hydrotris[3,5-bis(trifluoromethyl)pyrazol-1-yl]borato sodium ( $\text{Na}[\text{HB}(3,5-(\text{CF}_3)_2-\text{pz})_3]$ ) was prepared following a literature procedure.<sup>1</sup> Single-walled carbon nanotubes were purchased from SouthWest Nano Technologies (SWeNT® SG65, SWeNT® SG65-SRX, SWeNT® SG76, and SWeNT® CG100) or from Unidym (HIPCO® Super Purified). Cross-linked polystyrene particles (0.4-0.6  $\mu\text{m}$  diameter) were purchased from Spherotech and transferred from water into toluene. Dry toluene was purchased from J. T. Baker. All other chemicals were purchased from Sigma Aldrich and used as received. NMR spectra were recorded on Bruker Avance-400 spectrometers.

### 1.1 Synthesis of 1

8 mg (15.9  $\mu\text{mol}$ )  $[\text{CF}_3\text{SO}_3\text{Cu}]_2 \cdot \text{C}_6\text{H}_6$  were dissolved in 3 mL dry, degassed toluene. 17 mg (43.5  $\mu\text{mol}$ ) hydrotris[3,5-bis(trifluoromethyl)pyrazol-1-yl]borato sodium ( $\text{Na}[\text{HB}(3,5-(\text{CF}_3)_2-\text{pz})_3]$ ) were added, and the mixture was stirred for 14 h at r.t. The reaction mixture was filtrated through a syringe filter to receive a colorless solution of **1** with a concentration of ~6  $\mu\text{mol}/\text{mL}$  (6 mM).

The exact concentration of **1** was determined in the following way: A small amount of the solution was purged with ethylene for 20 min. The solvent was then evaporated, and the concentration of **1** determined by NMR spectroscopy using benzene as a reference for integration.

<sup>1</sup> H. V. R. Dias, W. Jin, H.-J. Kim, H.-L. Lu, *Inorg. Chem.* **1996**, *35*, 2317-2328.

## 1.2 Preparation of 1-SWNT

0.50 mg (41.6  $\mu\text{mol}$  carbon) of SWNTs were suspended in 0.8 mL dry *o*-dichlorobenzene, and 1.16 mL (6.9  $\mu\text{mol}$ ) of a 6 mM solution of **1** in toluene were added. The mixture was sonicated at 30 °C for 30 min. The resulting black dispersion of **1**-SWNT was used to prepare devices.

## 1.3 Preparation of 1-PS-SWNT

0.50 mg (41.6  $\mu\text{mol}$  carbon) of SWNTs were suspended in 0.8 mL dry *o*-dichlorobenzene, and 1.16 mL (6.9  $\mu\text{mol}$ ) of a 6 mM solution of **1** in toluene as well as 2.4  $\mu\text{L}$  of a suspension of cross-linked polystyrene particles in toluene (5  $\mu\text{g/mL}$ ) were added. The mixture was sonicated at 30 °C for 30 min. The resulting black dispersion of **1**-PS-SWNT was used to prepare devices.

## 2 Device preparation

Glass slides (VWR Microscope Slides) were cleaned by ultrasonication in acetone for 10 min, and after drying they were subjected to UV radiation in a UVO cleaner (Jelight Company Inc.) for 3 min. Using an aluminum mask, layers of chromium (10 nm) and gold (75 nm) were deposited leaving a 1 mm gap using a metal evaporator purchased from Angstrom Engineering.

Volumes of 1  $\mu\text{L}$  of the dispersion of **1**-SWNT was drop-cast in between the gold electrodes followed by drying in vacuum until a resistance of 1-5 k $\Omega$  was achieved.

## 3 Sensing Measurements

The devices were enclosed in a homemade Teflon gas flow chamber for sensing measurement (see Figure 1). The gold electrodes of the device are contacted with connections to the outside of the gas flow chamber, and two ports on opposite sides of the chamber allow to direct a continuous gas flow through the chamber.

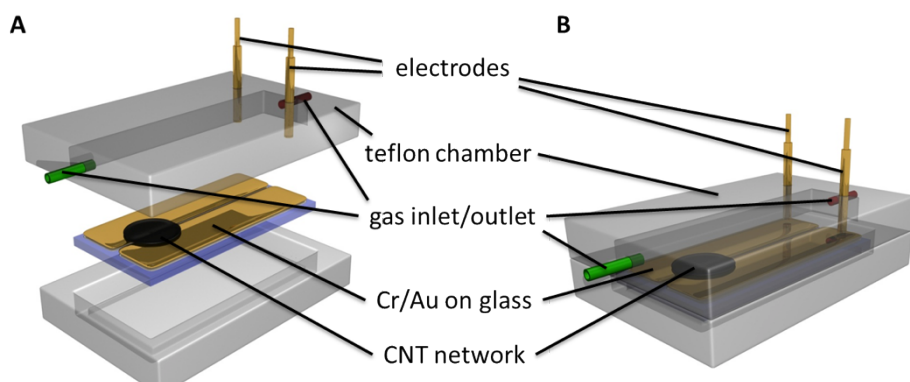


Figure 1. Gas flow chamber for sensing measurements.

The low concentration gas mixtures were produced using a KIN-TEK gas generator system. A trace amount of analyte emitted from a permeation tube is mixed with a nitrogen stream

(oven flow), which can be further diluted with nitrogen (dilution flow). For ethylene refillable permeation tubes were used, while for the solvents we performed calibration measurements ourselves by placing the solvent in the oven flow for set amounts of time. For fruit measurements the fruit was placed in a flow chamber, through which the “oven flow” was directed, which was then further diluted with nitrogen.

Electrochemical measurements were performed using an AUTOLAB instrument from Eco Chemie B.V. A constant bias voltage of 0.1 V was applied across the device, while current vs. time was measured. During the measurement the volume of gas flow over the device was held constant and switched between nitrogen and analyte/nitrogen.

## 4 FET measurements

As a substrate for FET measurements, a piece of silicon with a 300 nm  $\text{SiO}_2$  insulating layer onto which Au electrodes had been deposited, was chosen. Interdigitated electrodes with a 10  $\mu\text{m}$  gap were used. Analogous to the preparation of the devices for amperometric sensing measurements, dispersions of 1-SWNT and of pristine SWNTs were drop-cast between these electrodes.

For the measurements, the device was enclosed in a teflon chamber analogous to Figure 1 with an additional electrode to contact the Si bottom gate. The source-gate potential was swept from +2 V (+5 V in the case of 1-SWNT) to -20 V at a constant source-drain bias of 0.1 V and the chamber was flooded with nitrogen during the measurement. The source-drain current as well as the gate leakage current were recorded (Figure 2).

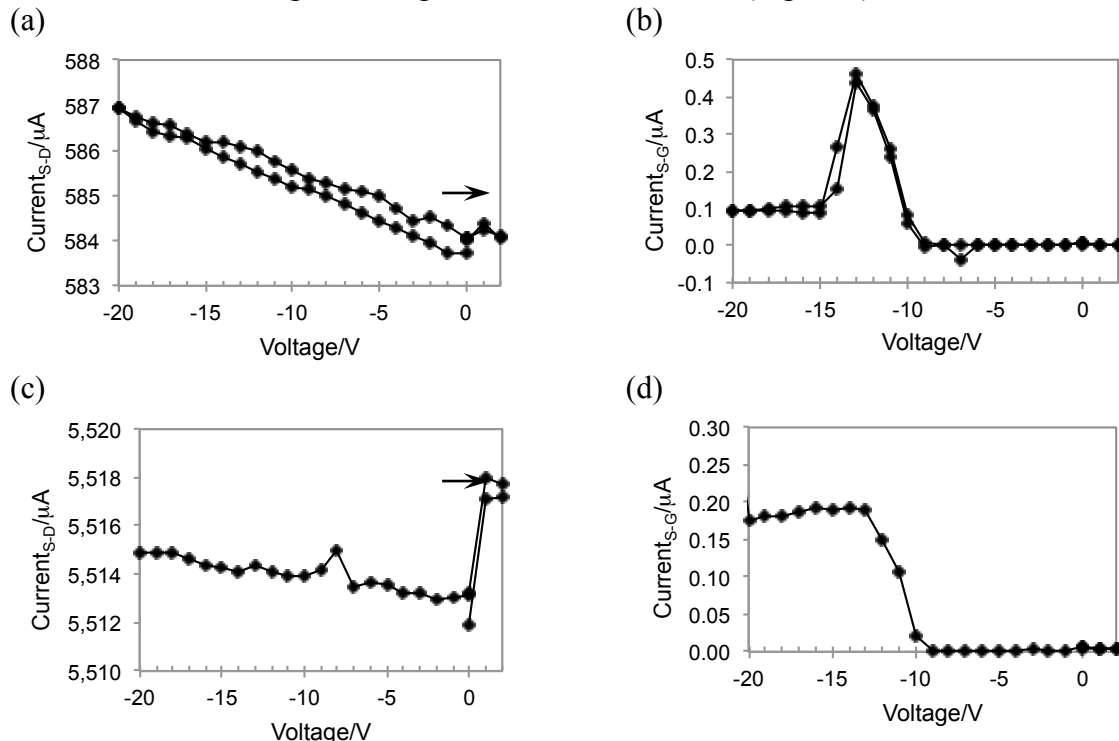


Figure 2. FET measurements: (a) Source-drain current and (b) gate leakage current for pristine SWNTs; (c) source-drain current and (d) gate leakage current for 1-SWNT. The voltage was swept from 0 to +2 V to -20V.

## 5 Testing of Different SWNT Types and Control Experiments

While optimizing sensitivity of the devices to ethylene, we tested different types of SWNTs. In Figure 3 (left) are shown the relative responses of devices made from different **1-SWNT** dispersions. The results of control experiments, in which dispersions of **2-SWNT**, **4-SWNT** (see below for structure of **4**) and SWNTs with  $[\text{Cu}(\text{CH}_3\text{CN})_4]\text{PF}_6$  were used to prepare devices are shown on the right in Figure 3.

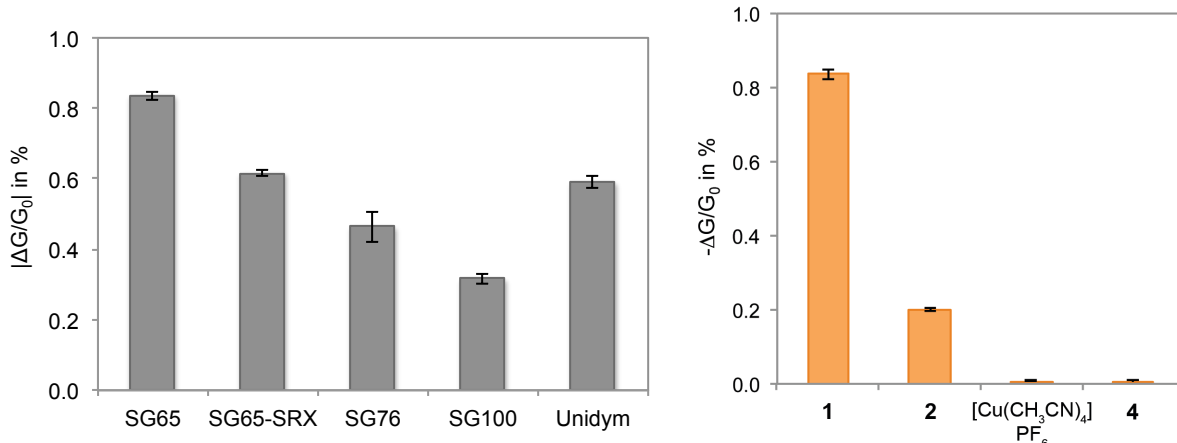
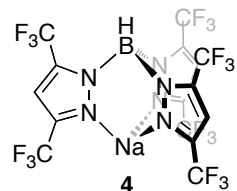


Figure 3. Responses to 20 ppm ethylene of (left) 1-SWNT devices made from different types of SWNTs and (right) devices made from 1-SWNT, 2-SWNT, SWNTs with  $[\text{Cu}(\text{CH}_3\text{CN})_4]\text{PF}_6$  and 4-SWNT.

## 6 Fruit Information

Fruit of the following types and weight was purchased from a Farmer's market:

Banana (Cavendish) – 142.5 g

Avocado (Hass) – 170.7 g

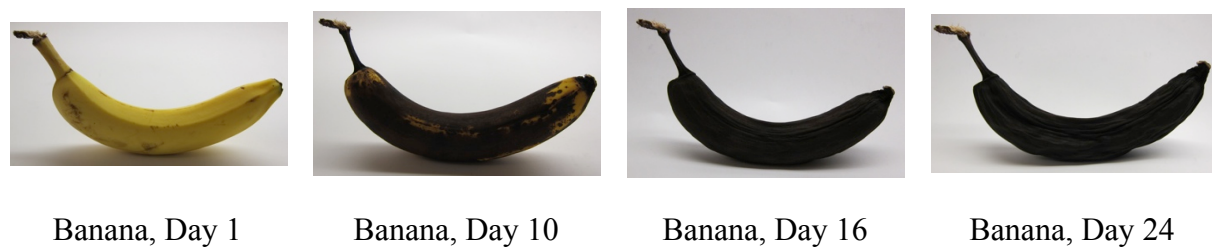
Apple 1 (Macintosh) – 119.1 g

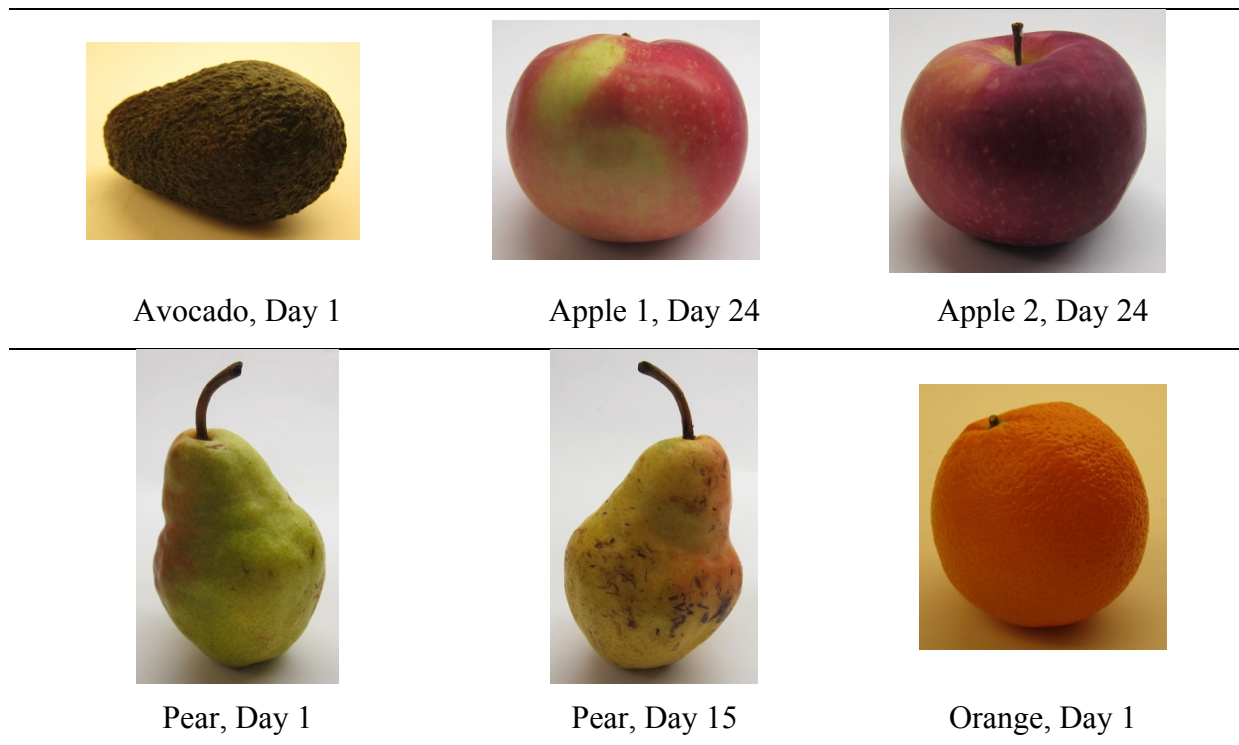
Apple 2 (Macintosh) – 111.3 g

Pear (Comice) – 246.1 g

Orange (Navel) – 265.0 g

Table 1. Pictures of fruit on different days of measurement.





## 7 Raman Measurements, IR Measurements, and XPS Data

IR spectra were recorded on a SMART iTR purchased from Thermo Scientific. The sample was dropcast onto a KBr card, and the spectrum measured in transmission mode.

Raman spectra were measured on a Horiba LabRAM HR Raman Spectrometer using excitation wavelengths of 785 nm and 532 nm. The samples were dropcast onto SiO<sub>2</sub>/Si substrates for the measurement.

XPS spectra (Figure 4) were recorded on a Kratos AXIS Ultra X-ray Photoelectron Spectrometer. The samples were drop-cast onto SiO<sub>2</sub>/Si substrates for the measurements. As the copper complex **1** is air sensitive, it was drop-cast under argon and the exposure to air was kept minimal (< 2 min) during the transfer into the XPS instrument. In the case of **1** and **2** sample charging was observed and a charge neutralizer was used. The resulting shift in energy was compensated by calibrating using the F 1s peak at 687 eV.

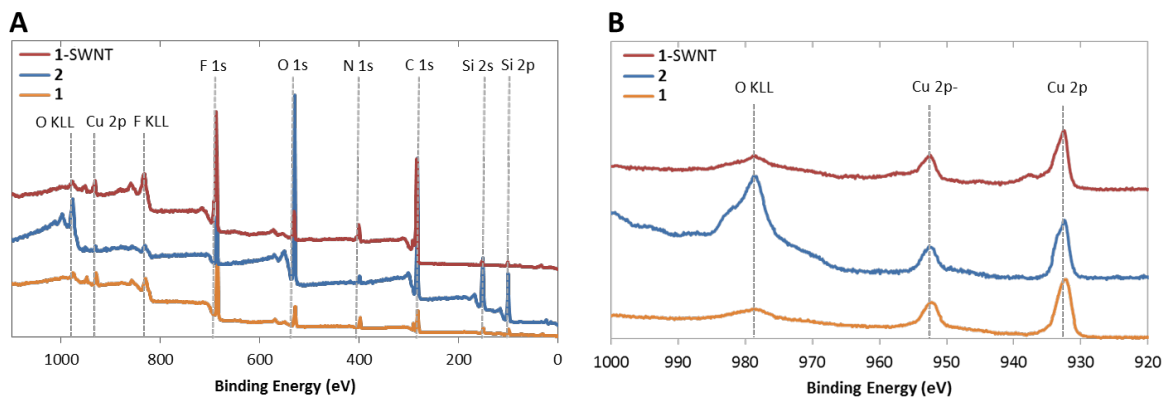


Figure 4. XPS measurements: (A) Survey scans of **1**, **2**, and **1**-SWNT and (B) high resolution scans of the Cu 2p region of **1**, **2**, and **1**-SWNT.

## 8 Scanning Electron Microscope Measurements

Scanning electron microscope (SEM) images were obtained on a JEOL 6700 scanning electron microscope.

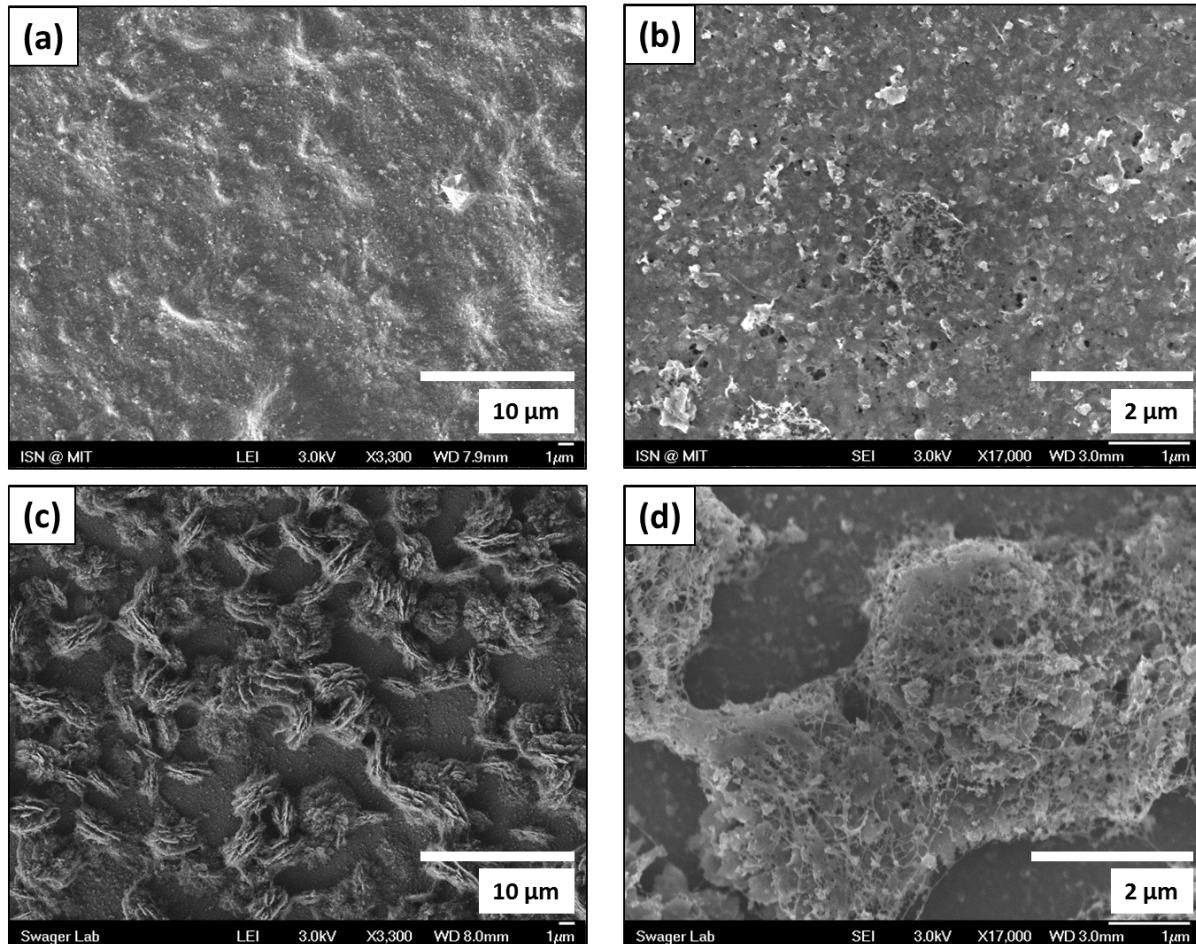
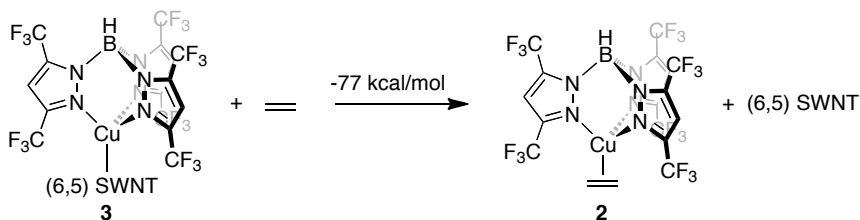


Figure 5. SEM images of **1**-SWNT devices: (a) **1**-SWNT drop-cast on glass at 3,300x magnification and (b) at 17,000x magnification; (c) **1**-SWNT with 5 weight-% cross-linked polystyrene beads drop-cast on glass at 3,300x magnification and (d) at 17,000x magnification.

Devices (prepared as described in device preparation) were analyzed by SEM, showing a relatively smooth film of **1**-SWNT on the glass substrate (Figure 5a and b). When 5 weight-% of cross-linked polystyrene beads (0.4-0.6  $\mu\text{m}$ ) were mixed with **1**-SWNTs before drop-casting, an increase of the surface roughness and thus the surface area can be observed (Figure 5c). At higher magnification, CNT bundles can be observed on the surface of the polymer as well as on the glass substrate (Figure 5d).

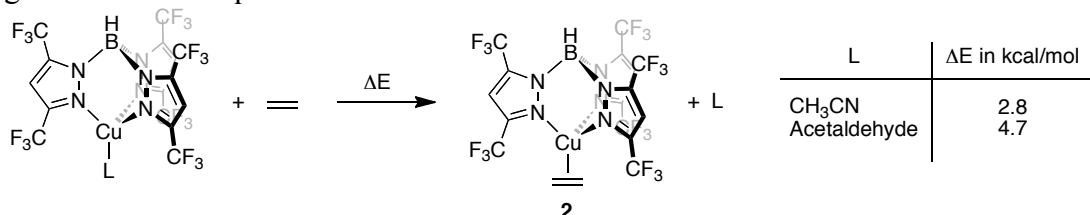
## 9 Isodesmic Equations

The isodesmic equation that allows comparing the binding strength of **1** to ethylene or an SWNT is shown in Scheme 1.



Scheme 1. Isodesmic equation to calculate the energy difference in binding of **1** to a (6,5) SWNT fragment or to ethylene (B3LYP/6-31G\*, LanL2DZ for Cu, no zero point correction).

The binding strengths of acetonitrile and acetaldehyde to **1** are compared to that of ethylene using the isodesmic equation in Scheme 2.



Scheme 2. Isodesmic equation to calculate the energy difference in binding of **1** to different ligands or to ethylene (B3LYP/6-31G\*, LanL2DZ for Cu, zero-point corrected).

## 10 Electronic and zero-point vibrational energies, Cartesian coordinates

Table 2. Electronic energies ( $\epsilon_0$ ), zero point vibrational energies (ZPVE), total energies ( $E_{\text{total}}$ ), and free energies G for all calculated structures (local minima) of Scheme 1 (B3LYP/6-31G\* for C, H, B, F, N, LanL2DZ for Cu).

Compound	$\epsilon_0$ [hartrees]	ZPVE [hartrees]	$E_{\text{total}}$ [kcal/mol]
<b>2</b>	-3000.31041	0.28383	-1882546.7
<b>3</b>	-7126.89966	-	-
Ethylene	-78.58746	0.05123	-49282.3
(6,5) SWNT fragment	-4205.29893	0.92740	-2638285.2
<b>1</b> -CH <sub>3</sub> CN	-3054.48032	0.27624	-1916543.6
CH <sub>3</sub> CN	-132.75493	0.04564	-83276.4
<b>1</b> -Acetaldehyde	-3075.54356	0.28639	-1929754.6
Acetaldehyde	-153.83012	0.05582	-96494.9

Table 3. Cartesian coordinates of all calculated structures (B3LYP/6-31G\* for C, H, B, F, N, LanL2DZ for Cu).

Structure	Cartesian coordinates					
	x	y	z	x	y	z
<b>2</b>	C -1.540089	2.586172	-0.246073	C 0.821251	-1.170186	2.786642
	N -0.797053	1.445453	-0.162164	C 2.179983	-1.347968	3.384780
	N 0.515430	1.748514	-0.242388	F 2.982690	-2.102775	2.597824
	C 0.592209	3.074148	-0.377046	C -2.823661	-1.297463	2.494495
	C -0.680595	3.660389	-0.386343	F -3.137567	-1.864751	3.676889
	B -1.243647	-0.035465	-0.001950	F 2.088497	-1.956475	4.580634
	N -0.669910	-0.880972	-1.184149	F 2.809496	-0.167436	3.569669
	N 0.664564	-1.026132	-1.349694	F -3.301237	-2.093315	1.517897
	C 0.836769	-1.810747	-2.418353	F -3.474141	-0.122215	2.418266
	C -0.391507	-2.188133	-2.970124	F -3.404404	-2.197236	-1.217046
	C -1.325145	-1.574069	-2.154166	F -3.363799	-0.427872	-2.479061

3	Cu	1.868976	-0.090400	0.021243	F	2.966300	-2.699379	-1.918789
	C	3.794181	0.269873	-0.713851	F	2.867271	-1.117814	-3.405999
	C	3.796375	0.446042	0.641679	F	-3.615558	1.938692	-1.176920
	C	2.200199	-2.182133	-2.907069	F	-3.443367	3.920101	-0.293330
	F	2.111667	-3.102398	-3.883889	F	1.743023	5.084711	-0.671928
	C	-2.816256	-1.643839	-2.294472	F	2.640510	3.295973	-1.533560
	F	-3.126423	-2.401893	-3.365805	H	-0.938828	4.702839	-0.480560
	C	1.913203	3.763088	-0.491752	H	-0.576097	-2.812482	-3.829189
	F	2.671562	3.595951	0.618168	H	-2.423682	-0.105957	0.004464
	C	-3.035745	2.639129	-0.183251	H	-0.596560	-1.954741	4.323817
	F	-3.510492	2.156712	0.982245	H	3.635875	1.425441	1.081869
	N	0.655135	-0.635520	1.572461	H	4.122743	-0.345545	1.307704
	N	-0.676406	-0.608643	1.337352	H	4.120372	-0.665261	-1.156013
	C	-1.335838	-1.134245	2.405059	H	3.631446	1.104491	-1.388897
	C	-0.407989	-1.506055	3.362040				
	C	5.622462	1.837865	-1.998145	C	-1.222750	-0.032613	-3.520534
	N	5.121506	0.953248	-1.134496	C	-5.954788	1.487901	1.234743
	N	6.146787	0.556808	-0.344415	C	-6.184745	1.432351	-0.175289
	C	7.283456	1.211782	-0.715353	C	-4.096143	1.294480	3.321321
	C	6.988696	2.048454	-1.774378	C	-2.733394	1.095901	3.699482
	B	6.003615	-0.663633	0.616447	C	0.849804	0.551022	1.810291
	N	5.586350	-1.890611	-0.257080	C	-0.082938	0.687007	2.881739
	N	4.568845	-1.795310	-1.139165	C	-5.413808	2.686047	1.797383
	C	4.592346	-2.909081	-1.878251	C	-4.492049	2.591123	2.867173
	C	5.612265	-3.769259	-1.458066	C	-0.493219	2.000618	3.271199
	C	6.216154	-3.081593	-0.419896	C	-1.836496	2.209005	3.663285
	C	3.673995	-3.098214	-3.042302	C	-2.354522	3.544422	3.646830
	F	3.051939	-1.943013	-3.378104	C	-1.461296	4.648788	3.693297
	C	7.384187	-3.542382	0.400695	C	-0.076675	4.431066	3.354092
	F	8.508136	-2.851921	0.122141	C	0.313260	3.132708	2.928479
	C	8.649700	0.973992	-0.139594	C	1.375191	1.738354	1.199175
	F	9.118700	-0.247250	-0.469386	C	1.284349	2.993829	1.882756
	C	4.786164	2.448034	-3.074837	C	-3.706244	3.739948	3.210590
	F	5.510024	2.597005	-4.202853	C	-2.964287	1.686509	-3.729524
	N	4.921824	-0.444906	1.717583	C	-1.589511	1.330355	-3.722553
	C	4.670318	0.610583	2.558764	C	-5.247505	2.342303	-2.245746
	C	3.920233	0.149708	3.622133	C	-5.817212	2.562146	-0.968273
	C	3.766846	-1.221063	3.351164	C	-5.484641	3.917331	1.065736
	N	4.369947	-1.573210	2.219658	C	-5.665462	3.850078	-0.354933
	C	5.128473	2.015487	2.348136	C	-4.505634	3.406000	-2.856961
	F	6.473852	2.115251	2.270103	C	-3.323569	3.072535	-3.595938
	C	3.092435	-2.238681	4.213833	C	-0.619717	2.363461	-3.523911
	F	3.921225	-2.712425	5.171997	C	-3.936934	0.676906	-3.494825
	C	1.253258	3.143413	-2.161055	C	0.944087	-0.695099	1.139042
	C	0.528335	2.062930	-2.737421	C	-5.018191	5.121424	1.659678
	C	0.724578	0.730217	-2.241359	C	-4.121158	5.031536	2.789476
	C	1.397753	0.547237	-0.971599	C	-5.344743	4.979253	-1.154181
	C	1.652916	1.738617	-0.185761	C	-4.723398	4.747696	-2.441959
	C	1.804934	2.997922	-0.849319	C	-3.336128	6.138075	3.245100
	C	1.189377	-0.702657	-0.278465	C	-2.052271	5.952810	3.692304
	C	0.762062	-1.853600	-1.019097	C	0.826608	5.502908	3.056619
	C	0.137540	-1.667510	-2.272824	C	1.769506	5.369721	2.072243
	C	-0.031322	-0.338514	-2.783848	C	1.858411	4.161059	1.305613
	C	0.616996	-3.119123	-0.353015	C	2.129883	4.163351	-0.103637
	C	0.276582	-4.276324	-1.096494	C	-2.372462	4.082482	-3.884591
	C	-0.408085	-4.090998	-2.369704	C	-0.957777	3.728920	-3.807704
	C	-0.634586	-2.747140	-2.814122	C	1.105284	4.448511	-2.718515
	C	-1.838720	-2.426419	-3.498950	C	0.031301	4.704051	-3.584041
	C	-2.823062	-3.436595	-3.663751	C	-2.833879	5.430044	-3.819361
	C	-2.434911	-4.805152	-3.530736	C	-3.977423	5.753706	-3.125562

	C	-1.203185	-5.108910	-2.935115	C	-5.290370	6.242068	-0.487075
	C	-4.207207	-3.085224	-3.573863	C	-5.140755	6.311746	0.876538
	C	-5.167693	-4.102360	-3.316844	C	2.337642	5.381102	-0.843792
	C	-4.776253	-5.460052	-3.601984	C	1.856455	5.516846	-2.113425
	C	-3.459133	-5.800605	-3.718299	F	2.719091	-4.019368	-2.803612
	C	-4.548169	-1.710574	-3.378907	F	2.032801	-1.687481	4.854837
	C	-5.668902	-1.389434	-2.576430	F	3.716809	1.671754	-3.369219
	C	-6.387229	-2.456532	-1.952008	F	4.323256	3.668680	-2.739106
	C	-6.278394	-3.781492	-2.465171	F	8.692472	1.077404	1.198678
	C	-6.880419	-2.252203	-0.620138	F	9.505908	1.886308	-0.649005
	C	-7.222166	-3.378616	0.174894	F	7.154593	-3.432890	1.719901
	C	-7.503398	-4.598536	-0.524653	F	7.631295	-4.841739	0.127553
	C	-7.055367	-4.790885	-1.804327	F	4.364021	-3.519987	-4.121388
	C	-6.670438	-0.978763	0.003144	F	2.648863	-3.296882	3.511571
	C	-6.396739	-0.932865	1.391037	F	4.722898	2.791724	3.372688
	C	-6.292335	-2.169838	2.107092	F	4.632590	2.563201	1.211854
	C	-6.891255	-3.345565	1.578061	Cu	3.361064	-0.199755	-1.080679
	C	-5.284503	-2.282160	3.121078	H	3.532893	0.722263	4.450227
	C	-4.874351	-3.570460	3.557487	H	5.881318	-4.736756	-1.851301
	C	-5.781231	-4.649792	3.310999	H	7.064170	-0.880782	1.106721
	C	-6.763851	-4.538605	2.359960	H	7.664486	2.694660	-2.311412
	C	-4.468175	-1.139535	3.408005	H	0.192286	-6.448471	-0.921685
	C	-3.106924	-1.337613	3.739588	H	0.001852	-6.479935	1.489346
	C	-2.586797	-2.672847	3.734049	H	-1.003866	-6.148382	-2.693674
	C	-3.473767	-3.777254	3.848985	H	-3.170465	-6.844097	-3.816206
	C	-1.252502	-2.878712	3.253274	H	-5.528541	-6.242585	-3.614418
	C	-0.839166	-4.182027	2.874354	H	0.691505	6.470769	3.529385
	C	-1.605651	-5.273090	3.388436	H	-1.235378	-6.288468	3.287247
	C	-2.878502	-5.077035	3.866448	H	-3.478139	-5.943757	4.125734
	C	-0.484943	-1.739560	2.840335	H	-5.618019	-5.612107	3.786200
	C	0.407212	-1.868870	1.750206	H	-7.349403	-5.416665	2.106654
	C	0.472960	-3.130017	1.071450	H	-7.968197	-5.427196	0.000656
	C	0.033691	-4.310399	1.726367	H	-7.175312	-5.767532	-2.262249
	C	0.256592	-5.509484	-0.380807	H	-3.707037	7.150845	3.121531
	C	0.148890	-5.527714	0.989929	H	-1.441983	6.823959	3.908184
	C	-4.896343	0.163820	3.004272	H	2.359800	6.234665	1.787611
	C	-5.862726	0.267977	1.957444	H	2.780026	6.239519	-0.348563
	C	-2.211487	-0.224398	3.705809	H	1.913281	6.476050	-2.621728
	C	-0.868582	-0.432803	3.264514	H	-2.214275	6.234128	-4.204314
	C	-6.359302	0.165778	-0.797252	H	-0.153004	5.737063	-3.862096
	C	-5.823870	-0.045850	-2.102857	H	-4.220999	6.801751	-2.982473
	C	-2.202027	-1.049571	-3.683023	H	-5.234117	7.158145	-1.066864
	C	-3.578258	-0.693239	-3.650596	H	-4.968622	7.280741	1.334214
	C	-5.096878	1.004816	-2.721795				
Ethylene	C	0.000000	0.000000	0.059709	H	-0.923279	0.000000	1.965006
	C	0.000000	0.000000	1.390291	H	-0.923279	0.000000	-0.515006
	H	0.923279	0.000000	-0.515006	H	0.923279	0.000000	1.965006
(6,5) SWNT fragment	C	6.220993	-3.565910	0.060834	C	-5.506331	3.610568	1.524063
	C	4.957003	-3.636169	-0.625896	C	-5.732309	3.679071	0.173269
	C	3.776555	-3.601432	0.177322	C	-1.534909	2.639686	2.789156
	C	3.850545	-3.109032	1.518379	C	-2.655745	2.011641	3.425333
	C	5.094196	-2.629422	2.013902	C	-3.968114	2.504861	3.193288
	C	6.284835	-3.068023	1.330279	C	0.663901	3.548115	1.233102
	C	2.631917	-2.769309	2.186722	C	0.896595	2.813516	2.435682
	C	1.386259	-3.270104	1.689337	C	-0.207571	2.198308	3.083775
	C	1.317780	-3.707580	0.336593	C	-0.024534	0.911336	3.676799
	C	2.510905	-3.682518	-0.461924	C	-1.175589	0.097692	3.906698
	C	4.848739	-3.422976	-2.007546	C	-2.475767	0.699854	3.973996
	C	3.613794	-3.064479	-2.584853	C	-3.612887	-0.104665	4.248903
	C	2.423228	-3.371567	-1.847556	C	-4.862697	0.574844	4.381398

1-CH <sub>3</sub> CN	C	1.137848	-3.019799	-2.374455	C	-5.033228	1.841100	3.877728
	C	-0.045912	-3.403567	-1.674650	C	1.262624	0.309555	3.638316
	C	0.048764	-3.782650	-0.296801	C	1.762802	3.763136	0.343824
	C	-1.135604	-3.814467	0.500158	C	1.533102	3.698797	-1.051178
	C	-1.065505	-3.411001	1.857909	C	2.224774	2.368501	2.726520
	C	0.177937	-2.952792	2.376353	C	2.410674	1.114287	3.354728
	C	0.174105	-1.859168	3.298859	C	1.174628	2.083621	-3.309171
	C	1.364422	-1.103251	3.467980	C	1.077912	0.774974	-3.839109
	C	2.621398	-1.660491	3.066725	C	1.066769	-1.979592	-3.336313
	C	3.824077	-0.902543	3.222649	C	2.286687	0.037790	-4.066771
	C	5.078961	-1.482008	2.877631	C	2.288295	-1.368046	-3.787155
	C	-1.078280	-1.298807	3.695386	C	2.653855	3.485340	-1.919106
	C	-2.286737	-2.049256	3.514900	C	2.474514	2.637219	-3.060978
	C	-2.287848	-3.115553	2.556579	C	3.106866	3.663860	0.831173
	C	-3.522361	-3.618098	2.073875	C	3.342523	2.974664	2.066436
	C	-3.611879	-3.962444	0.656987	C	3.715565	0.522329	3.347822
	C	-2.420694	-3.847786	-0.132950	C	3.966042	3.790021	-1.467108
	C	-2.508419	-3.404667	-1.482238	C	4.195893	3.913935	-0.045503
	C	-1.315144	-3.014386	-2.179619	C	4.855815	1.332343	3.100947
	C	-3.519550	-1.527262	3.991130	C	4.664518	2.585242	2.413608
	C	-4.670342	-2.351106	3.811800	C	5.504754	3.884493	0.532573
	C	-4.672054	-3.360379	2.877038	C	5.730924	3.250191	1.727002
	C	-3.774039	-3.006986	-1.989509	C	6.242031	-0.670850	3.096144
	C	-4.954720	-3.449224	-1.318583	C	6.134117	0.690203	3.194703
	C	-4.846589	-3.974270	-0.022611	C	3.523385	-2.045276	-3.627575
	C	-1.383896	-1.943659	-3.114349	C	3.519387	0.730285	-4.209152
	C	-2.630243	-1.261171	-3.287266	C	3.611743	2.085414	-3.707033
	C	-3.848334	-1.896114	-2.888732	C	5.031327	3.570181	-2.395229
	C	-5.092352	-1.231634	-3.071007	C	4.861438	2.738633	-3.474578
	C	-6.282301	-1.957922	-2.707431	C	4.671240	-0.068700	-4.474764
	C	-6.218266	-3.035423	-1.871166	C	4.673342	-1.413242	-4.185321
	C	-2.621337	0.140476	-3.481204	H	-5.606332	-3.870717	2.664142
	C	-3.824451	0.871444	-3.228356	H	-5.603085	-2.095837	4.304642
	C	-5.078679	0.195950	-3.227759	H	-5.766776	-4.142981	0.528146
	C	-0.176987	-1.321155	-3.546551	H	-7.131208	-3.501877	-1.509343
	C	-0.174476	0.090527	-3.784020	H	-7.253588	-1.579251	-3.009886
	C	-1.365128	0.826349	-3.544757	H	7.038744	1.289903	3.219202
	C	-1.264056	2.129334	-2.971985	H	-5.728623	0.043354	4.763583
	C	-2.412256	2.676741	-2.317259	H	-6.029200	2.272279	3.874851
	C	-3.716859	2.162885	-2.612588	H	-6.355134	3.638703	2.200308
	C	-4.857703	2.733584	-1.988096	H	-6.754151	3.757731	-0.183996
	C	-6.135209	2.227319	-2.395913	H	-7.040530	2.755337	-2.112874
	C	-6.242248	1.004514	-3.002850	H	-7.229988	0.593333	-3.185284
	C	-2.226240	3.434261	-1.136558	H	6.353031	4.258077	-0.032615
	C	-3.344209	3.616385	-0.259083	H	6.752555	3.136126	2.075235
	C	-4.666004	3.460137	-0.756873	H	7.229802	-1.117310	3.042814
	C	0.022990	2.665945	-2.697337	H	7.255923	-2.897858	1.784532
	C	0.205863	3.469920	-1.530045	H	7.133530	-3.783330	-0.488712
	C	-0.898398	3.667837	-0.658948	H	5.608110	-1.960283	-4.260336
	C	-0.665612	3.681556	0.750202	H	5.768684	-3.288968	-2.568282
	C	-1.764295	3.408938	1.623592	H	5.603889	0.403469	-4.766854
	C	-3.108629	3.574104	1.154462	H	5.727257	2.477589	-4.075133
	C	-4.197646	3.339607	2.035444	H	6.027167	3.939576	-2.171987
	C	1.558397	-1.028346	2.483303	C	-0.612768	-1.757627	-2.496412
	N	0.897801	-0.591049	1.349757	C	0.630747	-2.222392	-2.977240
	N	-0.454955	-0.747463	1.533715	C	1.567253	-1.643893	-2.121286
	C	-0.623853	-1.279975	2.767156	C	-1.970101	-2.056560	-3.030788
	C	0.617764	-1.476163	3.410209	F	-1.892607	-2.897532	-4.146537
	B	1.441151	-0.003769	0.002539	C	3.045673	-1.833488	-2.175358
	N	0.910243	1.461258	-0.161931	F	3.384363	-2.659790	-3.254730

	N	-0.440199	1.711362	-0.118142	F	3.408674	4.136247	-0.649215
	C	-0.597012	3.046953	-0.276603	F	3.762753	2.328233	0.639672
	C	0.650384	3.690072	-0.430713	F	-2.677061	3.405284	0.894945
	C	1.581729	2.655127	-0.352907	F	-1.866786	5.054864	-0.407960
	Cu	-1.686980	0.014756	-0.005932	F	3.755353	-0.638461	-2.342199
	N	-3.614861	0.008963	-0.009455	F	3.557977	-2.446265	-1.021959
	C	-4.786913	-0.002163	0.004164	F	-2.667843	-0.905858	-3.435416
	C	-6.249549	-0.018196	0.014521	F	-2.800597	-2.698694	-2.095236
	C	-1.952198	3.664030	-0.280162	F	3.556112	0.312865	2.634748
	F	-2.761091	3.208725	-1.337047	F	3.371197	-1.517228	3.930371
	C	3.061793	2.789599	-0.480634	F	-1.911070	-2.163070	4.562747
	F	3.576795	2.098569	-1.587888	F	-2.704806	-2.468921	2.476434
	C	-1.984258	-1.580661	3.292463	H	0.804923	-1.879065	4.391824
	F	-2.791366	-0.435552	3.417423	H	0.821619	-2.874896	-3.813157
	C	3.036897	-0.989917	2.676254	H	0.847009	4.739727	-0.573977
	F	3.743763	-1.732764	1.723496	H	2.623201	-0.008411	0.005039
	N	0.902560	-0.874732	-1.183603	H	-6.615736	-1.046912	-0.077463
	N	-0.448850	-0.951762	-1.420666	H	-6.625498	0.408106	0.951672
					H	-6.638799	0.572070	-0.822969
CH <sub>3</sub> CN	C	-0.007728	0.000000	-0.015213	H	-0.512483	0.888879	1.828660
	C	-0.001000	0.000000	1.445768	H	-0.512483	-0.888879	1.828660
	H	1.027085	0.000000	1.821660	N	-0.013567	0.000000	-1.175491
1-Acetaldehyde	C	1.482717	-1.553600	-2.185578	C	0.887426	3.667584	-0.278281
	N	0.851761	-0.844107	-1.208251	C	1.740746	2.581497	-0.182783
	N	-0.481901	-0.901456	-1.404399	C	-1.724337	3.767362	-0.298083
	C	-0.685136	-1.643932	-2.492532	F	-1.582769	5.070726	-0.614020
	C	0.527683	-2.088321	-3.034486	C	3.237781	2.609885	-0.159581
	B	1.430590	-0.049423	0.011845	F	3.664684	3.886821	-0.241505
	N	0.839914	-0.653319	1.329192	F	3.223842	-2.021133	3.687452
	N	-0.494976	-0.662014	1.526759	F	3.451315	-2.175473	1.527567
	C	-0.713842	-1.258615	2.698369	F	-2.929521	-1.946307	2.273669
	C	0.490795	-1.650367	3.296540	F	-2.140493	-2.197298	4.295030
	C	1.456397	-1.247609	2.388961	F	3.737195	2.081831	0.975952
	Cu	-1.575718	0.157531	-0.009444	F	3.776826	1.930763	-1.191596
	O	-3.571638	0.365553	0.058809	F	-2.357307	3.698493	0.891536
	C	-4.477573	-0.421054	-0.188148	F	-2.541373	3.201669	-1.212825
	C	-5.920591	-0.089088	0.018576	F	3.501025	-2.311238	-1.218041
	C	-2.110984	-1.401320	3.209358	F	3.265917	-2.450430	-3.378221
	F	-2.651876	-0.214394	3.550072	F	-2.084159	-2.502497	-4.159409
	C	2.939258	-1.415554	2.515962	F	-2.831344	-0.805480	-3.002953
	F	3.587246	-0.234465	2.495713	H	0.691617	-2.698648	-3.908107
	C	-2.079421	-1.927666	-2.944283	H	1.153307	4.709585	-0.355295
	F	-2.721583	-2.770016	-2.091953	H	0.642203	-2.150023	4.239956
	C	2.969270	-1.701885	-2.295550	H	2.610663	-0.129427	0.022531
	F	3.588492	-0.513499	-2.435519	H	-4.242294	-1.421638	-0.587405
	N	0.993474	1.444902	-0.103675	H	-6.365409	-0.818329	0.709162
	N	-0.317522	1.766288	-0.152654	H	-6.034093	0.920806	0.418064
	C	-0.390030	3.092830	-0.256795	H	-6.461271	-0.183661	-0.932062
Acetaldehyde	C	0.048448	-0.009446	-0.037783	H	0.843548	-0.638448	1.858059
	C	0.010636	-0.048011	1.469574	H	-0.942537	-0.476049	1.807055
	O	0.885150	-0.556557	-0.720470	H	0.056446	0.973729	1.869116
	H	-0.772644	0.576496	-0.511052				

## 11 Complete Gaussian Citation

Gaussian 03, Revision E.01, Frisch, M. J.; Trucks, G. W.; Schlegel, H. B.; Scuseria, G. E.; Robb, M. A.; Cheeseman, J. R.; Montgomery, Jr., J. A.; Vreven, T.; Kudin, K. N.; Burant, J. C.; Millam, J. M.; Iyengar, S. S.; Tomasi, J.; Barone, V.; Mennucci, B.; Cossi, M.; Scalmani, G.; Rega, N.; Petersson, G. A.; Nakatsuji, H.; Hada, M.; Ehara, M.; Toyota, K.; Fukuda, R.; Hasegawa, J.; Ishida, M.; Nakajima, T.; Honda, Y.; Kitao, O.; Nakai, H.; Klene, M.; Li, X.; Knox, J. E.; Hratchian, H. P.; Cross, J. B.; Bakken, V.; Adamo, C.; Jaramillo, J.; Gomperts, R.; Stratmann, R. E.; Yazyev, O.; Austin, A. J.; Cammi, R.; Pomelli, C.; Ochterski, J. W.; Ayala, P. Y.; Morokuma, K.; Voth, G. A.; Salvador, P.; Dannenberg, J. J.; Zakrzewski, V. G.; Dapprich, S.; Daniels, A. D.; Strain, M. C.; Farkas, O.; Malick, D. K.; Rabuck, A. D.; Raghavachari, K.; Foresman, J. B.; Ortiz, J. V.; Cui, Q.; Baboul, A. G.; Clifford, S.; Cioslowski, J.; Stefanov, B. B.; Liu, G.; Liashenko, A.; Piskorz, P.; Komaromi, I.; Martin, R. L.; Fox, D. J.; Keith, T.; Al-Laham, M. A.; Peng, C. Y.; Nanayakkara, A.; Challacombe, M.; Gill, P. M. W.; Johnson, B.; Chen, W.; Wong, M. W.; Gonzalez, C.; and Pople, J. A.; Gaussian, Inc., Wallingford CT, 2004.